RESEARCH ARTICLE

Asian Research Association

INTERNATIONAL RESEARCH JOURNAL OF MULTIDISCIPLINARY TECHNOVATION

DOI: 10.54392/irjmt2323

Comprehensive understanding of Methyl 2-Naphthyl Ether Molecule by Ab Initio Calculation method

A. Gokila [1, *]

[1] Department of Science and Humanities, Sri Eshwar College of Engineering, Coimbatore-641202, Tamil Nadu, India
*Corresponding author email: goki.giri@gmail.com
DOI: https://doi.org/10.54392/irjmt2323
Received: 05-12-2022; Revised: 17-01-2023; Accepted: 25-01-2023; Published: 13-02-2023

Abstract: The development of the geometrical structure and vibrational wave numbers of Methyl 2-Naphthyl Ether molecule (M2NE) are done with the help of ab initio HF- and Density functional method (DFT/B3LYP) of 6-31G(d, p) basis set. HF and DFT calculations optimize the geometric structure of the selected molecule. The B3LYP density functional method, with a base of 6-31G (d, p), is the best level of theory to repeat the expected wave numbers. Density functional theory was used to calculate the first hyperpolarization (β), electrical dipole moment (μ) of the examined molecule. The results of the calculations also show that a natural bond orbital (NBO) analysis of the M2NE could be performed. The FT-IR and FT-Raman spectrum were theoretically constructed for the title compound. There was a detailed understanding of FTIR and FT-Raman spectrum from experimental analysis. The considered HOMO and LUMO energies demonstrate that charge transfer takes place inside the molecule.

Keywords: Methyl 2-Naphthyl Ether, HOMO-LUMO, NBO analysis, Hyperpolarisability

1. Introduction

Naphthalene has been described as new class of potent antimicrobials against wide range of human pathogens. It occupies a central place among biologically active compounds owing to its varied and exciting antibiotic properties with less toxicity [1]. Numerous naphthalene containing antimicrobial drugs are existing like naftifine, nafacillin, terbinafine, tolnaftate, etc. that plays vital role against microbial infections [2, 3]. Further, the naphthalene derivatives like naproxen, nabumetone were also studied in depth as the nonsteroidal anti-inflammatory drugs (NSAIDs). They are mainly nonselective inhibitor of two cyclooxygenase (COX) isoform i.e., COX-1 and COX-2 [4, 5]. Moreover, the structurally relative naphthalene derivatives lower the parathyroid level by binding to calcium receptor on the parathyroid gland. Thus, it helps to regulate hyperparathyroidism especially in kidney disease or parathyroid gland neoplasm [6]. Based on the importance of naphthalene derivative as a main moiety for organic synthesis of several pharmaceutical drugs, it is advantageous to find out the alternate approach that can enhance the physicochemical and thermal properties of naphthalene derivative i.e., methyl-2-naphthyl ether (MNE). Recently, an alternate treatment approach i.e., healing therapy or therapeutic touch, known as the biofield energy treatment, which was reported in several fields. The National Institute of Health/National Center for Complementary and Alternative Medicine (NIH/NCCAM) conceived the biofield energy treatment in subcategory of energy therapies (putative energy fields) [7, 8]. The biofield treatment is being used in healing process to reduce pain, anxiety and to promote the overall health of human being [9, 10]. Biofield is an electromagneticfield that permeates and surrounds living organisms. This biologically produced electromagnetic and subtle energy field regulates the various physiological and communications functions within the human organism [11]. Researchers have attempted different biological studies and effects of biofield on various biomolecules such as proteins, antibiotics [12], bacterial cultures [13], and conformational change in DNA [14]. Prakash et al. reported that various scientific instruments such as Kirlian photography, resonance field imaging (RFI) and polycontrast interference photography (PIP) could be extensively used to measure the biofield of human body [15]. Thus, the human has the ability to harness the energy from the environment or Universe and transmit it to any living or nonliving object on the Globe. The object(s) receive the energy and respond into the useful way; this process is termed as biofield treatment. Recently, biofield energy treatment has been described as an alternative method to alter the physicochemical and thermal properties of several metals and ceramics [16-18]. It has also reported to alter the spectroscopic properties of various pharmaceutical drugs like paracetamol, piroxicam, metronidazole, and tinidazole [19, 20]. Moreover, the biofield treatment has been

studied in several fields like agriculture research [21, 22], biotechnology research [23], and microbiology research [24, 25].

Based on the published literature and outstanding impact of biofield energy treatment on various living and nonliving things, the present study was aimed to understand the structural and spectral properties of the Methyl 2-Naphthyl Ether molecule. In order to forecast its excitation wavelength, energy absorption, and oscillator strength (f), excitement of the synthesised molecule, the time-dependent density functional theory was applied for the theory of function. Electronic characteristics were also executed, such as energy gap, HOMO, LUMO and molecular electrostatic potentials. With DFT/B3LYP method, the vibrational waven numbers have been measured using the 6-31+G(d,p) basis set for molecular structure optimizations. Vibration studies were performed using the same basis set employed in the corresponding geometry optimizations. For the 3N- 6 freedom vibrational degrees, where N is the number of atoms in the system, the normal mode analysis of each structure did not produce imaginary frequencies. This indicates that at least a local minimum of the potential energy surface corresponds to the structure of each molecule. In the current study, this system was calculated using DFT method for optimized geometry, interaction energy and vibration frequencies, and NBO analyses were performed to conform the presence of hydrogen bonding between complexes [26]. An effective method for the study of intra- and inter-molecular bonding interaction between bonding also provides a convenient basis for the investigation of charging or conjugative interaction on molecular systems [27]. Our present work covers the quantitative and vibrational analysis of the Methyl 2-Naphthyl Ether molecule, based on our literature review using the DFT method.

2. Experimental Details

Methyl 2-Naphthyl Ether molecule (M2NE) with an affirmed purity greater than 98 percent, was bought from the Sigma–Aldrich Chemical Company (USA) and was used without additional purification. In the region of 400–4000 cm−1, the IFS 66V spectrophotometer with kBr pellet technology was used to report the FT-IR spectrum of the composite. With a scan speed of 30 cm−1 min−1 and a spectral resolution of 2.0 cm−1. The spectrum experiment was demonstrated at a room temperature. The Laser Raman spectra were recorded on the Brucker model IFS 66 V, with a spectroscope FRA 106 FT-Raman module accessory using 1064 nm Nd: YAG laser with the excitation wavelength in the region 400–4000 cm−1. The FT-IR and Laser-Raman experiments together with Raman and IR theoretical spectra are studied. Spectral measurements have been performed in the Government College of Technology, Coimbatore and Bharathiar University, India.

2.1 Computational details

The calculation of ab initio HF and DFT (B3LYP) was done with a GAUSSIAN 09w [28] programme package without any geometry restrictions [29]. The model of Methyl 2-Naphthyl Ether molecule (M2NE) was first optimised, and the resulting geometries were used as inputs for further calculations at Hf and DFT (B3LYP) levels in the prospective energy surfaces at the 6-31G (d, p) level. In the calculation of the vibrational occurrence at DFT level, optimised structures were used to minimise all stationary points. The vibrational frequency assignments were made with a high level of accuracy through the use of GAUSSVIEW [30] along with selected molecules.

3. Result and discussion

3.1 Geometric Structure

The optimized structure of the molecule and numbering of atoms of the molecule are obtained from Gaussian 09 and Gauss view program. Optimized geometrical parameters such as bond length, bond angles, and dihedral angles were calculated by HF/B3LYP using 6-31G (d.p) basic set. The obtained bond length, bond angle, dihedral angles are tabulated in supplementary table 1. The calculated B3LYP values are higher than HF values. Since the geometry of the molecular obtained by both basis sets were energetically most stable, the theoretical values of this method were taken for correlation and are more reliable. The C-C bond distances of naphthyl ether were in the range of 1.356 – 1.422 Å, whereas, the optimized C-C-C and C-C-H bond angles were in the range of 118.29 – 122.52◦ and 118.82 – 120.51◦ respectively. The C-O and C-H bond distances were calculated in the range 1.368–1.418Å and 1.073 and 1.086 Å respectively. The optimized C–H bond lengths in CH3 groups are computed by B3LYP method lies in the range 1.097A^0. The optimized structure will be given in figure 1. Further, the results of the calculations show that the calculated geometric parameter agree well with the remaining geometrical parameters. The structures optimized by B3LYP with poles apart base sets are almost identical to the ones tentatively observed. The developed bond length and bond angles are very close to the provisional values at all levels reported here.

These optimized parameters are slightly overestimated with crystallographic literature values. This overestimation can be explained that the theoretical calculations belong to isolated molecule in gaseous phase and the experimental results belong to similar molecule in solid state.

Table 1. Vibrational wave numbers obtained for methyl 2 naphthalene ether at HF and B3LYP/6-31G (d, p) [harmonic frequency (cm−1)]

Mode nos.	Experimental (cm^{-1})		Wavenumber (cm^{-1})				Vibrational Assignments
	FT-IR	FT-Raman	HF/6-31++G(d,p)	IR int	B3LYP/6-31++G(d,p)	IR int	
1			42	0.752	61	4.31	ν-OH
2		126	119	1.930	125	0.55	ν-OH
3			173	0.001	179	0.86	ν-OH
4			199	0.454	207	2.09	ν-OH
5			237	0.371	232	0.13	ν-OH
6			299	0.155	304	1.74	ν-CH
7		336	294	9.807	336	0.94	ν-CH + ν-CH + ν-CH
8		399	380	4.499	396	0.32	ν-CH + ν-CH + ν-CH
9			400	1.558	408	0.13	ν- CH + ν-CH
10	473		469	0.001	476	18.29	ν-CH
11			476	11.032	517	0.63	ν-CH
12		525	521	0.683	530	0.03	ν-OC
13			526	3.537	549	8.92	T- HCCO + β -HCH
14	615		594	0.809	622	5.24	β -HCH + β - HCH
15			636	0.572	644	0.32	β -HCH + β -HCH
16			670	0.965	703	10.03	ν-OC + ν-CC + ω - HCCO
17	735		741	0.282	748	21.04	ν-OC
18			742	0.757	749	11.32	ω - HCOC + ω - HCOC
19		777	744	52.763	771	0.56	δ -HCOC + T-HCOC + γ -HCH
20			805	0.163	804	38.96	ω -HCNC + ρ -HCOC + γ -HCO
21	822		849	0.494	852	25.93	γ - HCO + β -HCC
22			850	0.598	878	19.07	γ - HCO
23		938	916	3.176	940	0.06	β - HCO
24	953		955	1.720	952	2.94	β -HOC + β -HCC
25			965	6.132	958	4.38	ν- OC + β -HOC
26			969	0.370	981	0.05	ν-OC + ν-OC
27	1020		988	0.280	1029	7.55	γ - HOC
28		1043	1036	31.233	1058	47.22	ν-OC + β - HCO
29			1049	1.808	1139	27.10	β -HOC
30			1104	2.712	1156	0.80	β - HOC

31	1161		1133	1.981	1163	2.47	γ -HOC + ρ – HCCO
32			1136	2.362	1167	0.03	γ -HOC
33			1142	1.515	1178	87.19	ν-CO + S-PO
34	1204	1190	1156	13.812	1195	13.28	ν-CO
35	1258		1198	2.388	1246	32.81	ν-OC + ν-CC + ν-CO
36		1260	1224	7.736	1272	7.25	ω -HCOC +ν-PO
37			1254	0.099	1287	278.49	ν-OC + ν-OC
38	1373		1298	13.006	1373	12.12	ν-CO
39			1297	2.566	1388	4.63	ν-CO
40			1366	211.078	1397	0.18	ν- CO + ν-CO
41	1456		1414	53.765	1458	4.12	γ -OCOC + γ - OCO
42			1429	6.625	1462	9.68	β -CCO + ν-CC
43		1477	1445	16.754	1480	7.78	ν-CO + ν-CC + ν-CC
44			1451	46.584	1489	73.69	ω -HOCC
45			1454	23.027	1493	0.25	ω -HOPC + β - OCO
46		1549	1490	3.336	1536	69.13	τ - HOCC
47			916	3.176	940	0.06	γ -OCOC
48	1597		1571	47.816	1594	4.11	τ -HOCC + β -COC

IR int - IR intensity; Kmmol−1 w-weak; vw- very weak; s-strong; vs-very strong; m-medium; υ - stretching;β- in plane bending; γ- out-of –plane bending; ω – wagging; t- twisting; δ –scissoring; τ- torsion.

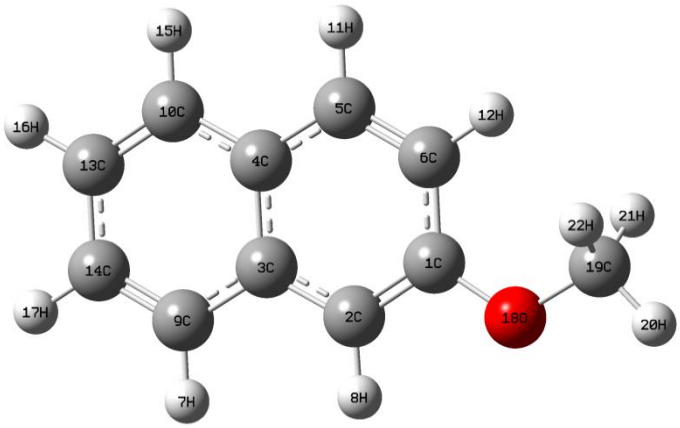

Figure 1. Optimized structure of Methyl 2 naphthalene ether by B3LYP/6-1G(d,p) basic set

C2–C6, C3–C7, C10–C9, C4–C8 and C5–C4 single-bond lengths are longer than the normal C–C single bond length of about 1.380˚ A. As a result of experimental findings and our calculations C6–C5, C1–C2, C7–C10 and C8–C9 bonds show typical double bond characteristics. C1–C2 bond length is relatively longer due to the electron-withdrawing effect. Optimized C–H bond lengths are clearly showing that the C–H bonds nearer to the methoxy group C5–H12 and C15–H16 having maximum variation with others. This is undoubtedly due to the impact of methoxy group. It is also evident by the farthest bond C2–H13 with maximum optimized bond length. The equilibrium structure for the ground state shows that the naphthalene ring is planar, and also the O atom and C, H atoms of methyl groups are lying approximately in the plane as evident from the torsional angles.

3.2 Vibrational spectral analysis

The vibrational analysis of Methyl 2-Naphthyl Ether was based on methyl, naphthyl, and ether modes characteristic vibration. HF and DFT theory (B3LYP and BLYP) with a 6-31 G (d, p) basis set were used for theoretical calculations. M2NE molecule consists 22 atoms therefore it has got 60 normal modes. It is in agreement with C_s point group symmetry, all vibrations are active both in Raman scattering and infrared absorption. The detailed vibrational assignment of the experimental wavenumbers is based on normal mode analyses and a comparison with theoretically scaled wavenumbers by different DFT methods. Since the scaled wavenumbers by following B3LYP/6-311G(d,p) method is found closest to experimental data than the results obtained using other methods, so only the report from this set of data are discussed in detail. The calculated wavenumbers are usually higher than the corresponding experimental quantities, due to the combination of electron correlation effects and basis set deficiencies. After applying, the different scaling factors, the theoretical wavenumbers are good in agreement with experimental wavenumbers. Table 1 presents the list of vibrational frequency and corresponding assignments of the title molecule. The FTIR and Raman spectra of M2NE molecule from both theoretical and experimental analysis are depicted in figure 2 -5, respectively.

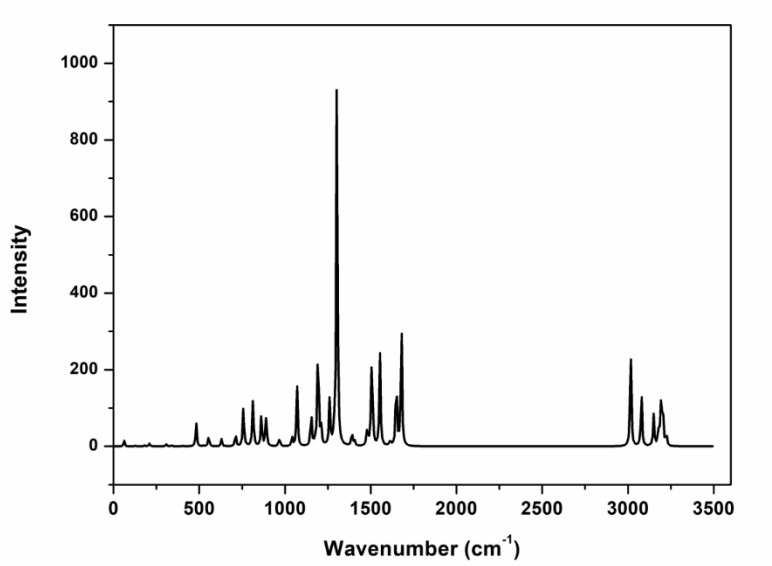

Figure 2. Theoretical FT-IR Spectrum of Methyl 2 naphthalene ether by B3LYP/6-311G(d,p) basic set.

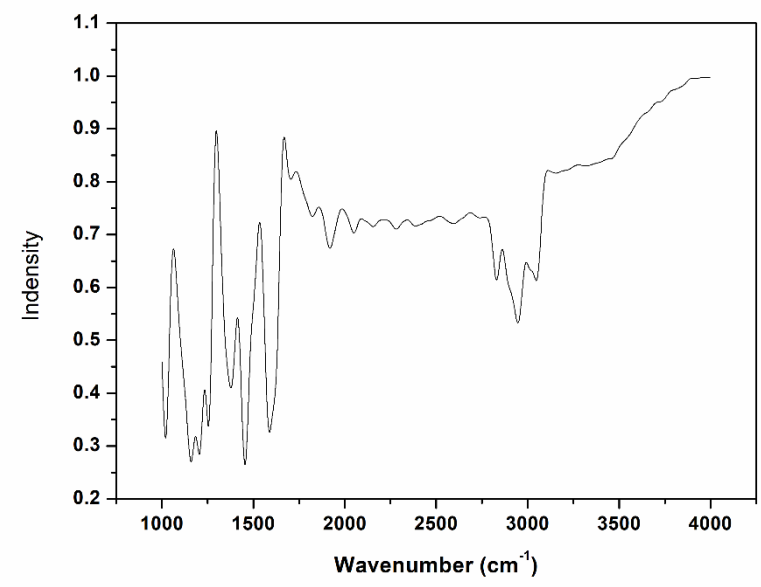

Figure 3. Experimental FT-IR of Methyl 2 naphthalene

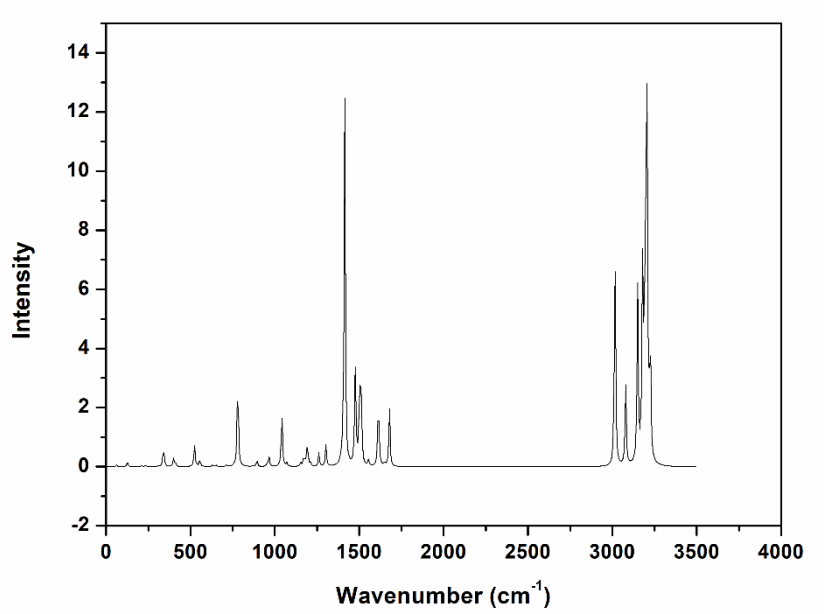

Figure 4. Theoretical FT-Raman of Methyl 2 naphthalene ether by B3LYP/6-311G(d,p) basic set.

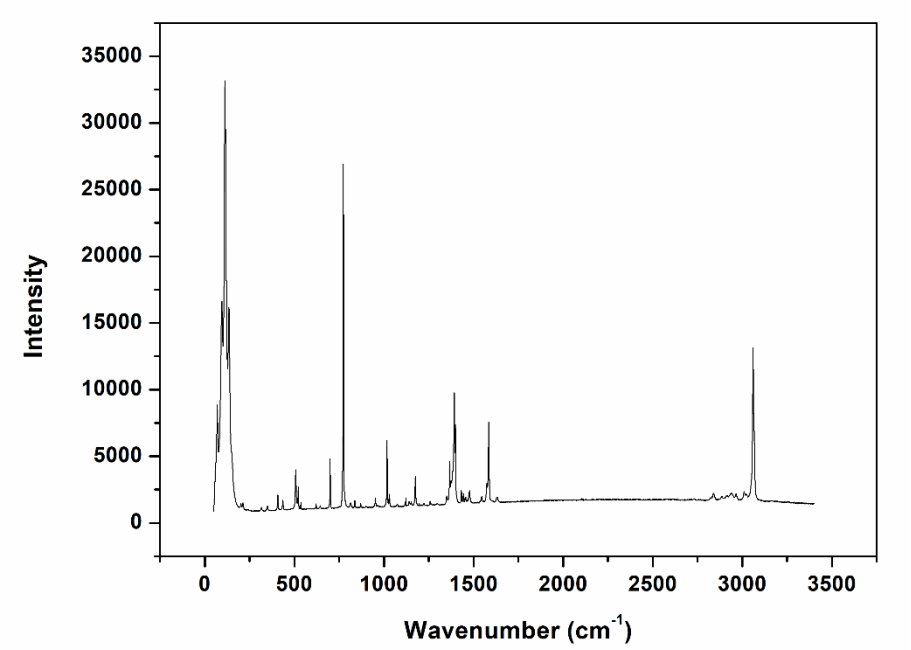

Figure 5. Experimental FT-Raman Spectrum of Methyl 2 naphthalene

C-H vibrations

The M2NE molecule causes C-H stretch; C-H bending vibrations are observed at the plane and C-H out of the plane. Based on the literature study the C-H vibration range in the 3050-3000 cm-1 region is the typical region for ready determination of C-H vibration range [26]. The title molecule has only one O–CH3 substitution in the naphthalene, hence is expected to give rise to seven C–H stretching vibrations due to naphthalene.

The expected C-H corresponds to stretching vibration for selected molecules (mode nos. 7-11). The vibrational mode nos (7-11) are assigned to the C-H stretching mode of title molecule computed by B3LYP/6-31G (d, p) method in 2997,2975,2969,2917,2873 and 2862 cm-1. They are good agreement with recorded FT-IR spectrum and FT-Raman spectrum. In the range of 2990-2861 cm-1, the same C-H stretching vibration was calculated with the method HF/6-31G (d, p).

In the region 1350-1470 cm-1, the C-H bending vibrations of methyl group and their plagiaristic fragments are observed. The strips are sharp but weak

to medium. The C-H bending vibrations computed by HF and B3LYP/6-31G (d, p) method explains good agreement with FT-IR spectral region at 1495-1394 cm-1. The same vibrations as the HF and B3LYP methods are also consistent with sample was measured. Overall, the theoretically developed vibrations of C-H stretch and bend are well in line with tentative values. All bands are medium intensity and in the expected region, but two vibrations are missing in the region due to overtone combinations. The change in the frequencies of these deformations from the values in benzene is determined mainly by the relative position of the substituents and is almost independent of their nature.

CO vibrations

The compound under study contains a C–O group and the absorption caused by such C–O stretching is generally very strong [31]. The C–O stretching vibrations of the light substituents [32] lie in the region 1095–1310 cm−1 and in carboxylic acids, the C–O stretching appear at 1725 with±65 cm−1 [33]. In this compound C–O stretching vibrations are observed at 1310 and 1260 cm−1with very weak intensity in infrared and Raman. The frequencies are certainly lesser than the cited values, which are quite expected as the bond is present between the naphthalene ring and methyl group. The C–O in-plane bending vibrations are observe dat 720 and 702 cm−1and out-of-plane bending vibrations at 398and 280 cm−1. All these vibrations are appeared with very weak intensity in Raman.

Methyl group vibration

Whenever a methyl group is present in a compound, it gives rise to two asymmetric and one symmetric stretching vibration. The asymmetric stretching for the CH3, NH2 and CH2 has magnitude higher than the symmetric stretching [34]. In the present case also two asymmetric vibration at 2990, 2940 cm−1 and one symmetric vibration at 2860 cm−1 are present which is in agreement with the literature [35]. The average frequency shift between asymmetric and symmetric stretching vibrations is found to be 105 cm−1. 2-Methoxy-1-naphthaldhyde shows methyl vibrations are in the range 2885–2803 cm^{-1}. This may indicate that the additional substitutions are pushes down the range of vibration. The asymmetric and symmetric stretching modes of methyl group attached the benzene ring are usually downshifted due to electronic effects and are expected near 2990, 2940 cm^{-1} asymmetric and 2860 cm^{-1} symmetric stretching vibration. This evident that the same electronic effect is also applicable in double ring compound like 1-methoxynaphthalene and the vibrations are observed at 2940 and 2865 cm $^{-1}$[36]. Moreover, the symmetrical bands are sharper than the asymmetrical bands. The same trend is also observed here. The large difference between the asymmetric and symmetric values has been attributed to the electronic effect. Thus, it is evident that the same electronic effect is also applicable in this compound. The CH3rocking and torsion vibrations are observed at 960 and 875 cm−1and at the lowest frequency 160 cm−1, respectively. The methyl group assignments proposed in this study is also in agreement with the literature values.

Table 2. Mullikan atomic charges obtained for methyl 2 naphthalene ether at HF and B3LYP/6-31G (d, p)

Atom	HF	DFT
C1	0.118542	0.406562
C2	-0.54221	-0.18916
C3	0.060854	0.00736
C4	0.184028	0.04579
C5	-0.60216	-0.12267
C6	0.727261	0.2134
H7	0.082176	0.153041
H8	0.120813	0.165482
C9	-0.3621	-0.13928
C10	-0.17744	-0.12349
H11	0.088209	0.157152
H12	0.097603	0.157876
C13	-0.01739	-0.16862
C14	-0.03928	-0.15082
H15	0.080544	0.150989
H16	0.110033	0.149371
H17	0.109662	0.151276
O18	-0.33809	-0.67216
C19	-0.17532	-0.02954
H20	0.154016	0.141372
H21	0.160128	0.114573
H22	0.160128	0.114575

Ring vibrations

Generally, the C=C stretching vibrations in benzene compounds form the bands in the region 1500–1650 cm −1 [37]. Several ring modes are affected by the substitution to the aromatic ring of naphthalene. In the present case, the C=C stretching bands are observed at 1550 and 1495 cm−1 with very strong intensities in infrared and 1640, 1580 and 1456 cm−1 with very weak and strong intensities in Raman. All these bands except the last one are in the expected range in IR and Raman. This indicate that the C=C modes are not affected by the substitutions. In this compound, the six C–C stretching vibrations are observed at 1440, 1435, 1425, 1417, 1220, 1190,1175 and 1182 cm−1. All these bands are

appeared with weak intensities expect one band and most of the bands are lie in the infrared region. The in-plane bending CCC vibrations generally occur at higher frequencies than of out-of-plane bending [38]. In the present study the bands are observed at 865 cm−1 with very weak intensity in Raman and in IR 845 and 840 cm−1 with medium and very weak intensity are assigned to C–C–C in-plane bending modes. The C–C–C out-of-plane bending wavenumbers are assigned at 500 cm−1 with very weak intensity in infrared and 430, 335, 220 and 195 cm−1 with very weak intensities in Raman. The maximum numbers of bands are observed in Raman. Some of the bands are missing in in-plane and out-of-plane bending which may due to heavy mass substitutions.

3.3 Mullikan Charge analysis

Effective atomic charge calculations have an important role in the application of quantum chemical calculation to molecular system because of atomic charges effect dipole moment, molecular polarizability, electronic structure, acidity–basicity behaviour and more a lot of properties of molecular systems [39]. Mulliken charge distributions were calculated by determining the electron population of each atom as defined by the basis sets. The calculated Mulliken charge values using various levels of theory and basis sets are listed in Table 2. The charge changes with basis set presumably occurs due to polarization. For example, the charge of O18 atom is−0.672 e−for B3LYP/6-31G (d,p),−0.338 e−for HF/6-31G (d,p). Considering the all methods and basis sets used in the atomic charge calculation, O18 and C19 atoms exhibit a substational negative charge, which are donor atoms. The figure 6 shows the comparison of Mullikan charge analysis calculated by both levels.

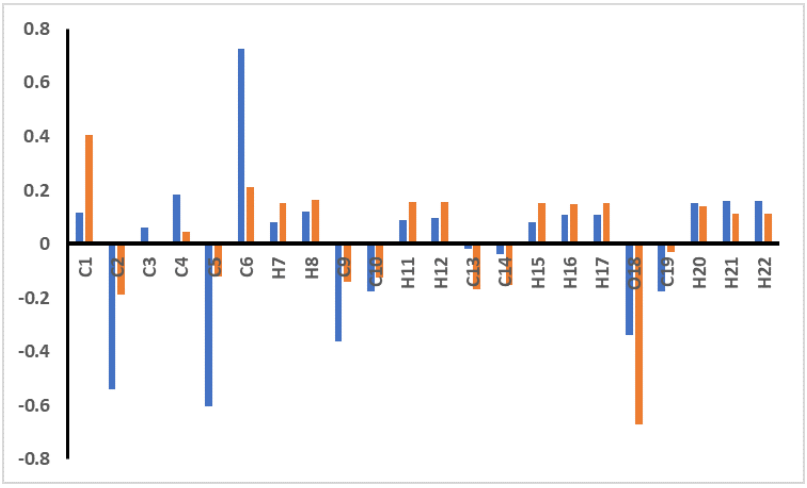

Figure 6. Mullikan's Atomic charges between theoretical (HF and DFT) approaches

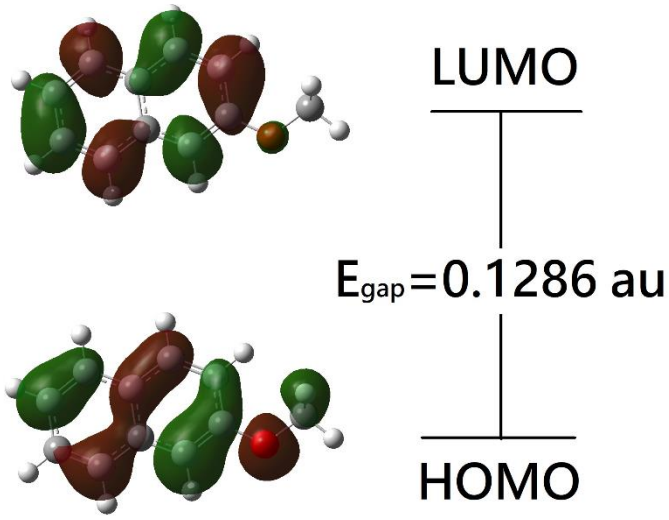

Figure 7. The molecular orbitals and energies for the HOMO and LUMO of Methyl 2 naphthalene ether by B3LYP/6-31G(d,p) basic set.

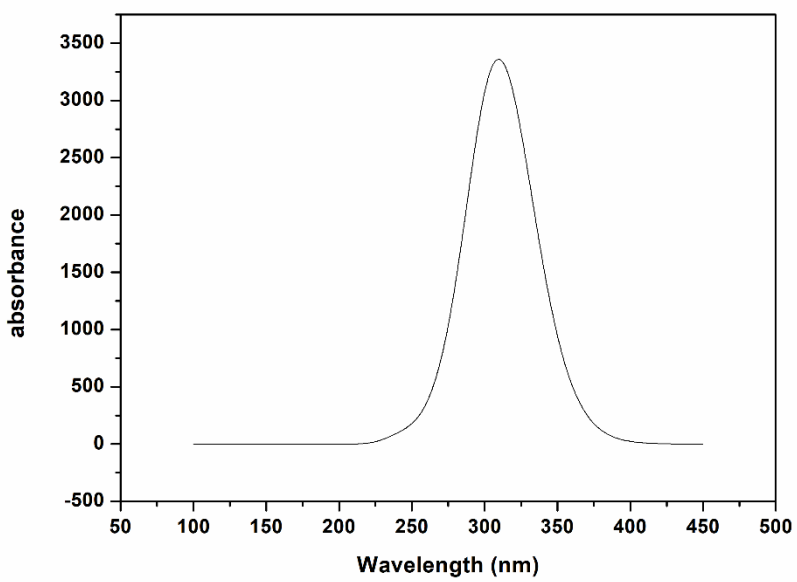

Figure 8. Theoretical UV–vis spectrum in ethanol for the title molecule calculated with the TD-HF/6-311++G (d, p) method

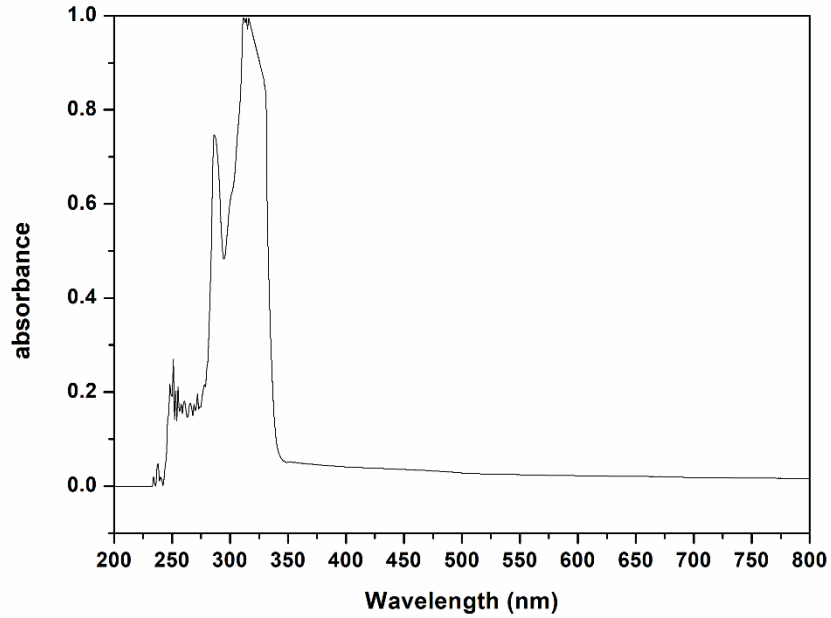

Figure 9. Experimental UV–vis spectrum in ethanol for Methyl 2 naphthalene ether

Table 3. Theoretical energy transition levels between HOMO and LUMO and frontier orbitals of methyl 2 naphthalene ether calculated by B3LYP/6-31++G (d,p) method

Level	MO Energy	Level	MO Energy	ΔE (eV)
HOMO	-0.20999	LUMO	-0.04716	4.428
HOMO	-0.20999	LUMO+1	-0.01166	5.394
HOMO	-0.20999	LUMO+2	-0.00120	5.744
HOMO-1	-0.24024	LUMO	-0.04716	5.254
HOMO-2	-0.28335	LUMO	-0.04716	6.427
HOMO-1	-0.24024	LUMO+2	-0.00120	6.570
HOMO-2	-0.28335	LUMO+2	-0.00120	7.743

Table 4. Experimental and computed absorption wavelength (λ), excitation energies (E) and oscillator strength (f) methyl 2 naphthalene ether calculated by B3LYP/6-31G (d,p) method

Exp wavelength (nm)	Theoretical wavelength (nm)	Excitedstate	Transition MO levels	Transition energy	Excitation energy	Oscillator strength
			41→43	0.1195		
318	311	I	41→44	0.1399	3.987	0.0798
			42→43	0.6680		
			42→44	-0.1279		
			41→43	0.5069		
295	279	II	42→43	-0.1815	4.443	0.0110
			42→44	-0.4508		
257	246	III	42→45	0.6953	5.031	0.0022

Table 5. Thermo dynamical parameter ofmethyl 2 naphthalene ether calculated by B3LYP/6-31G (d,p) method

Self-consistent field Energy (a.u.)		-500.283
Zero point energy (Kcal/Mol)		112.981
Rotational constant(GHZ)		0.47641
Rotational temperature (Kelvin)		0.02286
Energy (E) (KCal/Mol)	Translational	0.889
	Rotational	0.889
	Vibrational	117.146
	Total	118.924
Specific heat (C_v) (Cal/ Mol-Kelvin)	Translational	2.981
	Rotational	2.981
	Vibrational	32.166
	Total	38.127
Entropy(S) (Cal/ Mol-Kelvin)	Translational	41.083
	Rotational	30.428
	Vibrational	23.688
	Total	95.199
Dipole moment (Debye)		0.05188

3.4 HOMO and LUMO analysis

The homo and lumo orbitals are the energy bands that are most closely related to the energy of any pair of orbital fragments [40]. The reassignment of the intramolecular charge by the participant to an acceptable assembly in a single bond connection path can lead to large variations of molecular dipole. The molecular polarisation is to simultaneously strengthen the IR and Raman activity. It is also observed that the relative intentions in IR and Raman spectra are similar to that of the movement of electron cloud through a combined framework from a donor to electron acceptor groups. In addition, it can be found in the M2NE bands of the FT-IR spectrum. Ab initio calculations in conjugated systems which predict exceptionally large Raman and the Infra-red intensity on equal normal modes [41, 42].

Analysis of the wave function shows that the absorption of the electron is the transition from the ground to the first molecular orbital. One-electron excitation from the highest occupied molecular orbital (HOMO) to the lowest unoccupied molecular orbital is largely determined (LUMO). Theoretical energy transition levels between HOMO and LUMO and frontier orbitals of methyl 2 naphthalene ether calculated by B3LYP/6-31++G (d,p) method are listed in Table 3. The energy gap between the HOMO and LUMO of title molecule was calculated at the level of B3LYP/6-31 (d, p) and shows that the energy gap of the molecule reflects the chemical activity. LUMO symbolizes the ability to obtain an electron as an electron receiver; HOMO symbolizes that the electron is donated. The calculation at DFT/ B3LYP/6-31 (d, p) levels of the dimer HOMO – LUMO energy gap of Titled compound is shown in figure7.

3.5 Molecular orbital theory studies

Furthermore, the difference of energy band values is known to help us identify the chemical reactivity and stability of a molecule. A small band gap molecule is 29onization and the small gap is usually combined with a high reactivity of chemicals and a low kinetic stability. In terms of the degree of orbital reactivity of the atom [43] the quantium chemical calculations are performed. Mulliken was introduced a new formulation, which allowed to extend the concept to molecules, in terms of two further periodic properties, namely ionization potentials and affinity. The affinity of electron refers exactly to the ability of the legend to accept an electron. The big HOMO-LUMO gap means a hard molecule, and a small HOMO-LUMO gap means a soft molecule, due to its chemical hardness. The reactivity of the selected molecule is also associated with the molecule's hardness. The values of ionization and electron affinity are calculated with both HOMO and LUMO. For mulliken electron negativity, the mean HOMO and LUMO energy value can be used. The chemical potential is the negative of electronegativity. Softness is a molecular property that measures chemical reactivity. It's the contrary of durability. The index of electrophility is the measure of energy reduction due to the maximum electron flow between donor and recipient. The values of electronegativity, chemical potential, hardness value, chemical softness, and electrophilicity value are 0.1288 au, -0.1288 au, 0.0814 au, 6.1414 au and 0.1015 au, respectively, for the title Compound.

3.6 Electronic absorption

In order to understand electronic transitions of compound, DFT calculation on electronic absorption spectra in gas phase was performed. The computed electronic values, such as absorption wave length, excitation energies, and oscillator strengths are tabulated in Table 5. Figure 8 and 9 shows the absorbance spectrum of M2NE in theoretical and experimental analysis, respectively. As can be seen from Table 4 and Fig. 8-9, the calculated absorption maxima values have been found to be 318.The calculated band at 318 nm is predictedas $\pi \rightarrow \pi^*$ transition. According to the experimental and calculated results, the substance is colour less. Because, it does not show any absorbance invisible region (400–700 nm), in agreement with our UV–vis experiment and calculated oscillator strengths that are near zero. In view of calculated absorption spectra, the maximum absorption wavelength corresponds to the electronic transition from the highest occupied molecular orbital HOMO to lowest unoccupied molecular orbital LUMO with 83% contribution. The other wavelength, excitation energies, oscillator strength and calculated counterparts with major contributions can be seen in Table 5.

3.7 Thermodynamic properties

Several thermodynamic properties such as Zero Point Vibrational Energy (ZPVE), heat capacity (C_V), entropy (S) and rotational constants of the title compound have been calculated on the basis of vibrational analysis by density functional methods using 6-31G(d,p) basis set and are depicted in Table 5. The M2NE molecules has ZPVE as 118.924 K Cal mol^{-1}, CV as 38.127Cal $mol^{-1}K^{-1}$ and total thermal energy as 95.199K Cal mol^{-1}. These parameters can be used to calculate the other thermodynamic energies and estimate directions of chemical reactions in Thermo-chemical field according to relationships of thermodynamic functions and using second law of thermodynamics [44]. The thermodynamic data may provide useful information for the further study on title compound. The theoretical method has been used in static thermodynamic functions such as specific heat capacity, heat capacity and entropy changes at 297.8 ^oC.

3.8 Natural bonding analysis

The bonding NBOs are Lewis orbital and non-Lewis orbitals are antibinding NBOs. The complete Lewis orbits are supplemented by formally empty non-Lewis orbitals in an idea lised Lewis structure. The less electronic charge indicates strong effects of electron delocalization in Lewis orbitals. This NBO analysis provides more information on the communication between empty orbital and filled orbital, which could improve intra-molecular communication analysis. The stabilisation energy E (2), associated with the delocalisation (2e stabilisation) [45, 46], is estimates at the second order perturbation of NBO analysis of the Foc matrix in each of the donors NBO (i) and accepting power NBO (j).

$$E_{ij}^2 = \frac{qF_{ij}^2}{E_j - E_i}$$

For electron donor and electron acceptor communication, the value of E(2) greatly depends on the intensity of the interaction . The analysis by NBO is carried out on a titled molecule for the accounting and reporting of electron density within the molecule [47, 48]. The analysis will be performed to understand the intramolecular and rehybridization property. The transition from O 18 - C 19 to H22 is considered to give 0.112 kcal/mol, the strongest stabilization. The intramolecular communication between the hyper and the H→C-O binding orbital forms the overlap that results in the transfer of the communication charge which causes the stabilization of the fragment and its results are listed in supplementary table 2.

3.9 Hyperpolarizability calculations

The title molecular system's first hyperpolarizability (β0) and the related characteristics (β, α0 and α) were determined based on the finite field approach using the B3LYP/6-311G (d, p) basis set. The hyperpolarizability of Kleinman symmetry [49] is a third-rank tensor that can be described by the matrix 3 x 3 x 3, and the three-dimensional matrix can be reduced to 10 ingredients from 27 ingredients. As the coefficients for the Taylor series of energy expanses in the external electric field, the mechanisms of β are different.

$$E = E^0 - \mu_\alpha F_\alpha - 1/2\alpha_{\alpha\beta}F_\alpha F_\beta - 1/6\beta_{\alpha\beta\gamma}F_\alpha F_\beta F_\gamma + \cdots$$

Equation (1) shows a weak external electrical field and a uniform expansion, where E_0 is the energy of unperturbed part, $F_\alpha$the ground at the source μ_α, $\alpha_{\alpha\beta}$and $\beta_{\alpha\beta\gamma}$are the sections of the dipole moment, polarizability and the first hyperpolarizability, respectively. The total static dipole moment μ, the mean polarization α_0, the mean first hyperpolarizability β_0, is defined as

$$\mu = (\mu^2_x + \mu^2_y + \mu^2_z)^{1/2}$$

$$\alpha_0 = \frac{\alpha_{xx} + \alpha_{yy} + \alpha_{zz}}{3}$$

$$\alpha = 2^{-1/2}\left[(\alpha_{xx}-\alpha_{yy})^2 + (\alpha_{yy}-\alpha_{zz})^2 + (\alpha_{zz}-\alpha_{xx})^2 + 6\alpha^2_{xx}\right]^{1/2}$$

$$\beta_0 = (\beta^2_x + \beta^2_y + \beta^2_z)^{1/2}$$

$$\beta_x = \beta_{xxx} + \beta_{xyy} + \beta_{xzz}$$

$$\beta_y = \beta_{yyy} + \beta_{xxy} + \beta_{yzz}$$

$$\beta_z = \beta_{zzz} + \beta_{xxz} + \beta_{yyz}$$

The calculated first hyperpolarizability of M2NE for B3LYP/6-31G (d, p) method is 62.019X 10^{-30}esu and the values are listed in Table 8 and 9.

4. Conclusion

The FTIR and FT-Raman spectra of the molecular structure were carried out. The Equilibrium geometries, harmonic frequencies of M2NE have been identified and analysed at the theory of ab initio HF and DFT. The fact that the calculations have been performed on a single molecule in the gaseous state against the tentative values in the presence of intermolecular communication may cause any divergence between the observe frequencies and the worked-out frequencies. The gap between wavenumber values observed and scaled is very small in most fundamental values. The tasks performed at DFT theoretical level therefore appear to be correct with reasonable differences from the tentative values. The FT-IR spectrum, theoretically developed, coincides with the FT-IR spectrum observed. The DFT theory developed the two different forward-looking energy scans of the hydroxyl group. The DFT system was employed using 6-31G (d, p) to understand the electric dipole and the first order hyperpolarizability of the selected molecule. An analysis of HOMO-LUMO energy and density distribution was conducted for M2NE molecule. DFT/B3LYP technique was performed for the NBO analysis of M2NE. Natural bonding analysis was used to determine the stabilization energy. This study shows that calculations from DFT/B3LYP are a powerful way to understand organic molecules for various potential applications.

References

[1] Y.B. Rokade, R.Z. Sayyed, Naphthalene derivatives: A new range of antimicrobials with high therapeutic value, Rasayan Journal of Chemistry, 2(4) (2009) 972-980.

[2] C.O. Wilson, O. Gisvolds, J.H. Block, J.M. Beale, (2004) Textbook of organic medicinal and pharmaceutical chemistry. Lippincott, Williams and Wilkins, Philadelphia.

[3] Y. Rokade, N. Dongare, Synthesis and antimicrobial activity of someazetidinone derivatives with the naphthol, Rasayan Journal of Chemistry, 3(4) (2010) 641-645.

[4] A.B. Pandya, D.G. Prajapati, S.S. Pandya Synthesis of novel naphthalene COX inhibitors for anti-inflammatory activity, Journal of Applied Pharmaceutical Science, 2(8) (2012) 226-232. https://doi.org/10.7324/JAPS.2012.2840

[5] V. Cavrini, P. Roveri, R. Gatti, C. Ferruzzi, A.M. Panico, M.S. Pappalardo, Synthesis of 2-methoxynaphthalene derivatives as potential anti-inflammatory agents Il Farmaco; Edizione Scientifica, 37(3) (1982) 171-178. https://doi.org/10.1002/chin.198234159

[6] D. Lednicer, (2007) The organic chemistry of drug synthesis. John Wiley & Sons INC., Hoboken, New Jersey, USA. https://doi.org/10.1002/9780470180679

[7] M. Koithan, Introducing Complementary and Alternative Therapies, Journal for Nurse

Practitioners, 5(1) (2009) 18-20. https://doi.org/10.1016/j.nurpra.2008.10.012

[8] J. Hok, C. Tishelman, A. Ploner, A. Forss, T. Falkenberg, Mapping patterns of complementary and alternative medicine use in cancer: an explorative crosssectional study of individuals with reported positive "exceptional" experiences, BMC Complementary Medicine and Therapies, 8 (2008) 48. https://doi.org/10.1186/1472-6882-8-48

[9] D. Aldridge, Spirituality, healing and medicine, British Journal of General Practice, 41(351) (1991) 425-427.

[10] M. Cahil, (1999) Nurses handbook of complementary and alternative therapies, Springhouse Corporation, Springhouse, PA.

[11] Z. Movaffaghi, M. Farsi, Biofield therapies: biophysical basis and biological regulations?, Complementary Therapies in Clinical Practice, 15(1) (2009) 35-37. https://doi.org/10.1016/j.ctcp.2008.07.001

[12] D.J. Benor, Survey of spiritual healing research. Complememtary Medical Research, 4(1) (1990) 9-33.

[13] B. Rubik, A.J. Brooks, G.E. Schwartz, In vitro effect of Reiki treatment on bacterial cultures: Role of experimental context and practitioner well-being. The Journal of Alternative and Complementary Medicine, 12(1) (2006) 7-13. https://doi.org/10.1089/acm.2006.12.7

[14] G. Rein, The in vitro effect of bioenergy on the conformational states of human DNA in aqueous solutions. Acupuncture & Electro-Therapeutics Research, 20(3-4) (1995) 173-180. https://doi.org/10.3727/036012995816357005

[15] S. Prakash, A.R. Chowdhury, A. Gupta, Monitoring the human health by measuring the biofield "aura": An overview, International Journal of Applied Engineering Research, 10(35) (2015) 27654-27658.

[16] M.K. Trivedi, S. Patil, R.M. Tallapragada, Effect of biofield treatment on the physical and thermal characteristics of silicon, tin and lead powders, Journal of Material Sciences & Engineering, 3(2) (2013) 125. https://doi.org/10.4172/2169-0022.1000125

[17] M.K. Trivedi, R.M. Tallapragada, A. Branton, D. Trivedi, G. Nayak, O. Latiyal, S. Jana, (2015) Potential impact of biofield treatment on atomic and physical characteristics of magnesium, Vitamins & Minerals, 4(3) 129.

[18] M.K. Trivedi, G. Nayak, S. Patil, R.M. Tallapragada, O. Latiyal Evaluation of biofield treatment on physical, atomic and structural characteristics of manganese (II, III) oxide, Journal of Material Sciences & Engineering, 4(4) (2015).

[19] M.K. Trivedi, S. Patil, H. Shettigar, K. Bairwa, S. Jana, Effect of biofield treatment on spectral properties of paracetamol and piroxicam, Chemical Sciences Journal, 6 (2015) 98. https://doi.org/10.4172/2150-3494.100098

[20] M.K. Trivedi, S. Patil, H. Shettigar, K. Bairwa, S. Jana, Spectroscopic characterization of biofield treated metronidazole and tinidazole, Medicinal Chemistry, 5 (2015) 340-344.

[21] F. Sances, E. Flora, S. Patil, A. Spence, V. Shinde, Impact of biofield treatment on ginseng and organic blueberry yield. Agrivita Journal of Agricultural Science, 35(1) (2013) 22-29. https://doi.org/10.17503/Agrivita-2013-35-1-p022-029

[22] V. Shinde, F. Sances, S. Patil, A. Spence, Impact of biofield treatment on growth and yield of lettuce and tomato, Australian Journal of Basic and Applied Sciences, 10(6) (2012) 100-105.

[23] S.A. Patil, G.B. Nayak, S.S. Barve, R.P. Tembe, R.R. Khan, Impact of biofield treatment on growth and anatomical characteristics of Pogostemoncablin (Benth.), Biotechnology, 11(2012) 154-162. https://doi.org/10.3923/biotech.2012.154.162

[24] M.K. Trivedi, S. Patil, H. Shettigar, M. Gangwar, S. Jana, Antimicrobial sensitivity pattern of Pseudomonas fluorescens after biofield treatment, Journal of Infectious Diseases & Therapy, 3(2015) 222. https://doi.org/10.4172/2332-0877.1000222

[25] M.K. Trivedi, S. Patil, H. Shettigar, S.C. Mondal, S. Jana, Evaluation of biofield modality on viral load of Hepatitis B and C viruses, Journal of Antivirals & Antiretrovirals, 7(2015) 83-88. https://doi.org/10.4172/jaa.1000123

[26] L. Turker, S. Gumus, T. Atalar, A DFT Study on Nitro Derivatives of Pyridine, Journal of Energetic Mterials, 28(2) (2010) 139-171. https://doi.org/10.1080/07370650903273224

[27] Mohanbabu, B., Bharathikannan, R. & Siva, G. Investigations on structural, optical, electrical, mechanical and third-order nonlinear behaviour of 3-aminopyridinium 2,4-dinitrophenolate single crystal, Applied Physics A, 123 649 (2017). https://doi.org/10.1007/s00339-017-1262-1

[28] M.J. Frisch, G.W. Trucks, H.B. Schlegel, G.E. Scuseria, M.A. Robb, J.R. Cheeseman, G. Scalmani, V. Barone, B. Mennucci, G.A.

Petersson, H. Nakatsuji, (2009) Gaussian, Inc., Gaussian 09, Revision A. 1, Wallingford CT.

[29] H.B. Schlegel (1982), Optimization of equilibrium geometries and transition structures, Journal of Computational Chemistry, 3(2), 214-218. https://doi.org/10.1002/jcc.540030212

[30] R. Dennington, T. Keith, J. Millam, (2009), Gauss View, version 5, Semichem Inc., Shawnee Mission KS.

[31] M. Chalasinski, M. Szczesnaik, Origins of Structure and Energetics of van der Waals Clusters from ab Initio Calculations, Chemical Reviews, 94 (7) (1994) 1723-1765. https://doi.org/10.1021/cr00031a001

[32] J.A. Pople, A.P. Scolt, M.W. Wong, L. Radom, Scaling Factors for Obtaining Fundamental Vibrational Frequencies and Zero-Point Energies from HF/6–31G* and MP2/6–31G* Harmonic Frequencies, Israel Journal of Chemistry, 33 (1993) 345-350. https://doi.org/10.1002/ijch.199300041

[33] A. Raj, K. Raju, Hema Tresa Varghese, C.M. Granadeiro, H.I.S. Nogueira, C.Y. Panicker, IR, Raman and SERS Spectra of 2-(Methoxycarbonylmethylsulfanyl)-3,5-dinitrobenzene Carboxylic Acid, Journal of the Brazilian Chemical Society, (2009) 549-559.

[34] D. Lin-Vien, N.B. Colthup, W.G. Fateley, J.G. Grasselli, (1991) The Handbook of Infrared Raman Characteristic Frequencies of Organic Molecules, Academic Press, Boston, MA.

[35] S.J. Bunce, H.G. Edwards, A.F. Johnson, I.R. Lewis, P.H. Turner, Synthetic polyisoprenes studied by Fourier transform Raman spectroscopy, Spectrochimica Acta Part A: Molecular Spectroscopy, 49(5-6) (1993) 775-783. https://doi.org/10.1016/0584-8539(93)80102-G

[36] J. Mohan, (2001) Organic Spectroscopy-Principles and Applications, 2nd ed., Narosa Publishing House, New Delhi, India.

[37] G. Varasanyi, (1969) Vibrational Spectra of Benzene Derivatives, Academic Press, New York, USA.

[38] G. Socrates, (2001) Infrared and Raman Characteristic Group Frequencies, 3rd ed., John Wiley & Sons Ltd., Chichester, UK.

[39] Mulliken R S, J Chem, Electronic Population Analysis on LCAO-MO Molecular Wave Functions. I, The Journal of Chemical Physics, 231833 (1955) 135-141. https://doi.org/10.1063/1.1740588

[40] F. De Proft, P Geerlings, Conceptual and computational DFT in the study of aromaticity, Chemical reviews, 101(5) (2001) 1451-1464. https://doi.org/10.1021/cr9903205

[41] B. Lakshmaiah & G. Ramana Rao, Vibrational analysis of substituted anisoles, I-Vibrational spectra and normal coordinate analysis of some fluoro and chloro compounds, Journal of Raman spectroscopy, 20(7) (1989) 439-448. https://doi.org/10.1002/jrs.1250200709

[42] M. Govindarajan, M. Karabacak, A. Suvitha, S. Periandy, FT-IR, FT-Raman, ab initio, HF and DFT studies, NBO, HOMO-LUMO and electronic structure calculations on 4-chloro-3-nitrotoluene, Spectrochimica Acta Part A: Molecular and Biomolecular Spectroscopy, 89(2012) 137-148. https://doi.org/10.1016/j.saa.2011.12.067

[43] B. Mohanbabu, R. Bharathikannan, G. Siva, Structural, optical, dielectric, mechanical and Z-scan NLO studies of charge transfer complex crystal: 3-aminopyridinum-4-hydroxy benzoate, Journal of Materials Science: Materials in Electronics, 28, (2017) 13740-13749. https://doi.org/10.1007/s10854-017-7218-6

[44] N.M. Brown, R.J. Turner & D.G. Walmsley, Inelastic electron tunnelling spectroscopy of some 1-and 2-substituted adamantanes on plasma-grown aluminium oxide, Journal of the Chemical Society, Faraday Transactions 1: Physical Chemistry in Condensed Phases, 77(10) (1981) 2481-2491. https://doi.org/10.1039/f19817702481

[45] S. Ghammamy and A. Lashgari, Structural Properties, Natural Bond Orbital, Theory Functional Calculations (DFT) and Energies for the 3-Methyl-4-(2-phenyl-1,2, 4-triazolo-[1,5-a]pyrimidin-7-yl)furazan Compound, Middle-East Journal of Scientific Research 17 (8) (2012)1080-1086.

[46] A.E. Reed F Weinhold, Natural bond orbital analysis of near-Hartree-Fock water dimer, The Journal of Chemical Physics, 78 (1983) 4066-73. https://doi.org/10.1063/1.445134

[47] A.K. Srivastava, N. Misra, Theoretical investigation on the structure, stability and superhalogen properties of OsF n (n= 1-7) species, Journal of Fluorine Chemistry, 158(2014) 65-68. https://doi.org/10.1016/j.jfluchem.2013.12.008

[48] N. Prabavathi, A. Nilufer and V. Krishnakumar, Quantum mechanical study of the structure and spectroscopic (FT-IR, FT-Raman, 13C, 1H and UV), NBO and HOMO-LUMO analysis of 2-quinoxaline carboxylic acid, Spectrochimica Acta Part A: Molecular and Biomolecular

Spectroscopy, 92(2012) 325-335. https://doi.org/10.1016/j.saa.2012.02.105

[49] D.A. Kleinman, Nonlinear dielectric polarization in optical media, Physical Review, 126(6) (1962) 1977. https://doi.org/10.1103/PhysRev.126.1977

Acknowledgement
None

Conflict of interest
The Author has no conflicts of interest to declare that they are relevant to the content of this article.

Does this article screened for similarity?
Yes